AJTEC2011-44390

STEAM-METHANE REFORMING IN A MICROCHANNEL UNDER CONSTANT AND VARIABLE AXIAL SURFACE TEMPERATURE PROFILES

Benn Eilers
Oregon State University
Corvallis, Oregon, USA

Vinod Narayanan*
Oregon State University
Corvallis, Oregon, USA
*vinod.narayanan@oregonstate.edu

Sourabh Apte
Oregon State University
Corvallis, Oregon, USA

John Schmitt
Oregon State University
Corvallis, Oregon, USA

ABSTRACT

An experimental study of steam methane reforming in a microchannel is presented. Palladium nanoparticles, deposited on a porous aluminized FeCrAlY felt, served as catalyst sites for the reforming reactions. Parametric studies of steam-methane ratio, residence time, average reactor temperature, and temperature distribution were performed. Results demonstrated in excess 60 percent conversion of methane at an average reactor temperature of 900°C and the lowest experimented residence time of 26 milliseconds. Methane conversion was found to be strongly dependent on reactor temperature. Ramping temperature distributions demonstrated a 46 percent greater hydrogen output than isothermal reactions performed at the same average temperature.
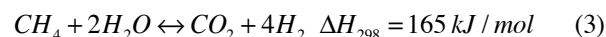
NOMENCLATURE

h height (m)
l length (m)
$\dot{M}_i$ molar flow rate of component i (mole/min)
M_i molecular weight of component i (kg/kmol)
$\dot{m}_i$ mass flow rate of component i (g/min)
P pressure (kPa)
R_{SM} molar steam-methane ratio $(mol/s)_{H2O}/(mol/s)_{CH4}$
t_{res} residence time (s)
T temperature (°C)
U average velocity (m/s), uncertainty (%)
$\dot{V}$ volumetric flow rate (m³/s)
w width (m)
X_i molar fraction of component i
Y_i mass fraction of component i

ΔH_{298} enthalpy change of reaction (kJ/mol)
ρ_i density of component i (kg/m3)
μ dynamic viscosity (kg/m-s)

INTRODUCTION

Hydrogen has been investigated extensively as an alternative energy carrier due to the lack of CO_2 production during combustion and the ability to generate energy directly using fuel cells. Hydrogen can be produced using a variety of methods including electrolysis, thermolysis, partial oxidation, and steam reforming. Of these options, steam reforming of methane is the most economical and most widely used method of hydrogen generation [1,2]. Steam-methane reforming is a well understood industrial process used for generating hydrogen and synthesis gas. This process has been used for over 70 years, with the majority of hydrogen produced being used for ammonia production [3]. Steam-methane reforming involves the following three reactions

$$CH_4 + H_2O \leftrightarrow CO + 3H_2 \qquad \Delta H_{298} = 206 \, kJ/mol \quad (1)$$
$$CO + H_2O \leftrightarrow CO_2 + H_2 \qquad \Delta H_{298} = -41 \, kJ/mol \quad (2)$$
$$CH_4 + 2H_2O \leftrightarrow CO_2 + 4H_2 \quad \Delta H_{298} = 165 \, kJ/mol \quad (3)$$

The general configuration of a large-scale facility consists of reforming tubes several meters long oriented vertically and heated with side-fired burners, with residence times on the order of one second. In order for large steam-methane reforming plants to operate efficiently, it is necessary to

increase the pressure to the range of 2000 – 4000 kPa [4]. The corresponding density increase of the reacting mixture allows for smaller reforming equipment, thereby reducing capital investment. Equilibrium methane conversion is higher for a given temperature at lower pressures, necessitating an increase in reaction temperature in the larger scale facilities to achieve high hydrogen yield. Typical operating temperatures range from 900 ^{o}C to 1050 ^{o}C.

By performing the reforming reaction in mini- and micro-reactors, it is possible to take advantage of increased heat transfer rates and low diffusion times allowing equipment size and residence times to be decreased by an order of magnitude. The decreased residence times present in a microreactor can also be used to suppress undesirable slower reactions such as coke formation [5]. The benefits of using microchannels do not come without significant drawbacks, as outlined by Holladay et al. [6]. However, coke formation is more of an issue in microchannels. The pressure drop through the channel is greatly increased and can be quickly exacerbated through coke formation. Sealing the small devices is a non-trivial issue with very few researchers reporting on techniques of assuring a completely sealed system. Thermal management in small reactors becomes difficult at elevated temperatures due to the large size of the connectors relative to the channel. System monitoring requires specialized techniques and equipment to accurately characterize operational parameters. Very small flow

rates of reactants must be stably fed to the reactor, requiring precise instrumentation. Additionally, small diameter thermocouples must be used to minimize conduction losses where appropriate. Despite the aforementioned drawbacks, microchannel technology has been shown to greatly reduce the conversion time in steam-methane reforming.

Table 1 summarizes the literature on experiments in mini/microchannel steam-methane reforming. All of the above mentioned literature on microchannel steam-methane reforming helped guide the research efforts discussed herein by providing insights into experimental design and the expected responses to parametric variations. Experimental work of steam-methane reforming in a microchannel is limited to research conducted by Pacific Northwest National Laboratory (PNNL, Richland, WA) [9,12], collaborations of Velocys, Inc (Plain City, OH) with PNNL [7, 8, 11] and work by Alkhaldi [10].

Tonkovich et al. [7] explored long term steam-methane reforming at high pressures (1400 kPa) in a 250 μm channel at residence times of 4.3 and 6 ms. Thermal energy for the reaction was provided by an integrated co-flow combustion chamber adjacent to the reaction zone. The catalyst bed was located on the wall adjacent to the combustion chamber. The catalyst used in this experiment was Rh on a mixture of MgO and Al_2O_3 subsequently deposited on a FeCrAlY felt material. The above catalyst was the same as what was used in all work conducted by PNNL and Velocys Inc. shown in Table 1 with

TABLE 1. SUMMARY OF EXPERIMENTAL STUDIES ON MICROCHANNEL STEAM-METHANE REFORMING

Reference	Reactor	Catalyst	Test Conditions	Details / Findings
Tonkovich et al. [7]	Inconel w=9.65 mm l=177.8 mm h=250 μm	Rh on MgO/Al_2O_3 on FeCrAlY Felt	T = 870°C P = 1300 kPa R_{SM} = 3 & 4.8 t_{res} = 4.3 & 6 ms	Parallel flow combustion channels Long duration testing (568 h) ~90% conv observed q" = 17.7 - 18.2 W/cm^2
Wang et al. [8]	Inconel w=8.9 mm l=50.8 mm h=889 μm	Rh on MgO/Al_2O_3 on FeCrAlY Felt	T = 650 - 900°C P = 101 kPa R_{SM} = 1 - 3 t_{res} = 25 - 27 ms	FeCrAlY preferable CAT support Stable conv for 40 h. (R_{SM}=1, T=900°C) ↑% conv with ↑R_{SM} ↑% conv linear to ↑T
Cao et al. (2005) [9]	Inconel w=9 mm l=51 mm h=250 μm	Rh on MgO/Al_2O_3 on FeCrAlY Felt	T = 850°C P = 405 - 2027 kPa R_{SM} = 2 t_{res} = 3.8 & 13.8 ms	2 CAT orientations tested 74% conv (P=405 kPa t_{res}=3.8 ms) 93% conv (P=405 kPa t_{res}=13.8 ms) ↓% conv with ↑P
Alkhaldi (2005) [10]	Inconel w=22 mm l=75 mm h=250 μm	Pd on aluminized FeAl	T = 630 - 1000°C P = 101 kPa R_{SM} = 4.8 - 8.1 t_{res} = 27 - 42 ms	10% conv (T=630°C, t_{res}=39ms) 49% conv (T=1000°C, t_{res}=27ms) ↑% conv with ↑R_{SM} ↑ CO selectivity with ↑T 24% ↓ in activity after 100 min R_{SM} >1.39 to prevent coking
Tonkovich et al. (2007) [11]	Inconel w=10.7 mm l=11.4 mm h=76 μm	Rh on MgO/Al_2O_3 on FeCrAlY Felt	T = 811 - 837°C P = 1140 - 1290 kPa R_{SM} = 3 t_{res} = 90 & 900 μs	Crossflow combustion channels 21.3% conv @ 90 μs 99% conv @ 900 μs Stable conv after 100 h.
Johnson et al. (2007) [12]	Inconel w=9.4 mm l=50.8 mm h=390 μm	Rh on porous Al_2O_3	T = 540 - 900°C P = 101 kPa R_{SM} = 1 t_{res} = 27 ms	10% ↓ in conv after 100 h. @ 900°C only ↑5% conv w 3X ↑ CAT loading ↑ sintering with ↑CAT loading No coking @ R_{SM} = 1
Eilers et al. (this work)	304 SS w=19 mm l=133 mm h=700-1067 mm	Pd on aluminized FeCrAlY	T=625-925 ^{o}C P=103-201 kPa R_{SM} = 2.54 - 5.8 T_{res}=5.3 – 42.5 ms	62% conv (T=904°C, R_{SM}=2.9, t_{res}=26ms) ↑% conv linear to ↑ t_{res} ↑% conv exponential to ↑T No observed R_{SM} dependence

the exception of the work by Johnson et al. [12] who used a porous Al_2O_3 substrate. Long-term testing results indicated conversion rates of around 90 percent with slight deactivation of the catalyst.

A modified design of the integrated combustor /reformer unit was examined by Tonkovich et al. [11]. Multiple cylindrical combustion chambers were situated in a cross-flow configuration to the steam-methane reforming flow. A 0.28 mm thick catalyst bed was located adjacent to the wall with the combustion chambers and formed an open channel height of 76 µm. This reactor was also tested at high pressures (1300 kPa), but with very low residence times of less than 1 ms. Time series conversion data was presented for testing at a residence time of 0.09 ms which indicated methane conversion percentages between 16 percent and 19 percent for over 100 hr of testing, suggesting little to no catalyst deactivation.

The reactors used in Wang et al. [8], Cao et al. [9] and Johnson et al. [12] all had similar width and length dimensions (9 mm and 51 mm) but had different channel heights. The reactors were heated in a furnace to isothermal conditions. Wang et al. [8] examined the effects of low steam-methane ratios (1 -3) in a microchannel height with a height of 889 µm that was filled entirely with the porous catalyst bed. All tests were carried out at atmospheric pressure. The steam-methane ratio variations were conducted at a fixed temperature of 900°C and residence time of 27 ms. The conversion of methane was greatly reduced at small steam-methane ratios, but no carbon was formed on the catalyst after testing under these conditions for 40 hours. Wang et al. [8] also tested two different catalyst beds at multiple temperatures. The first catalyst bed was of a powder form, and the second bed was an aluminized FeCrAlY catalyst bed. Tests were performed with a steam-methane ratio of unity, a reactor pressure of 101 kPa, and residence time of 27 ms. The FeCrAlY catalyst bed provided increased methane conversion at all temperatures tested.

The reactor used in Cao et al. [9] was configured to have two 250-µm-thick catalyzed FeCrAlY inserts on either walls of a microchannel, with an open channel gap of 250 µm. Tests were performed at temperature of 850°C with a steam-methane ratio of 2. Two different residence times were tested over a range of pressures. It was seen that increased pressure had a strong negative effect on methane conversion percentage. Cao et al. [9] also looked at an unconventional catalyst bed configuration whereby the catalyst coated FeCrAlY was arranged in a saw-tooth pattern through the reactor. This caused the reacting flow to be forced through the catalyst bed multiple times. Modeling and experiments demonstrated increased methane conversion using the conventional design of the catalyst beds confined to the walls.

The reactor of Johnson et al. [12] used a Rh catalyst on a porous ceramic. Two different catalyst loadings were tested in this configuration, one with 3.7% Rh weight loading, and another with 10% Rh weight loading. Experiments were performed with a steam-methane ratio of 1 and a residence time of 27 ms and a reactor temperature of 900°C. The results of 100 hours of testing on each catalyst bed revealed a counter-intuitive result indicating higher conversion for the lower loading of catalyst. Post-testing microstructural analysis of both catalyst beds revealed increased sintering of the catalyst bed with the higher loading, suggesting that there is an ideal loading density to maximize methane conversion.

Alkhaldi [10] used Pd as a catalyst on an aluminized FeAl substrate. Experiments were performed at atmospheric pressure and methane conversions at temperatures ranging from 630 – 1000°C with steam-methane ratios of 4.8 – 8.1. Changes in density of the flow were not accounted for during the testing, causing the residence time to vary. Residence times for these experiments ranged from 27 – 42 ms, with higher steam-methane ratios having larger residence times at a given temperature. Similarly, for a given steam-methane ratio, higher temperatures produced smaller residence times. The data as they are presented suggest a slight increase in methane conversion with an increase in steam-methane ratio. There is also a strong positive correlation between methane conversion percentages with reactor temperature.

This paper presents experimental results of reforming in a mini/microchannel under constant and variable temperature profiles. The motivation behind this work lies in the use of solar energy, which is a clean and renewable energy source, to provide the necessary heat for the endothermic reactions (Eqs. 1 and 3). Since the temperatures for reforming are typically high, a parabolic dish solar collector with a microchannel receiver at its focal region could be used for solar-thermal reforming, thus providing a cleaner pathway for hydrogen production. In such receiver chemical reactors, it is expected that the heat flux and temperature distribution is non-uniform. This study presents a *first step* in characterizing reforming performance of such solar reactors under such variable temperature conditions. The design of the minichannel was such that the non-uniform heat flux profile expected inside of a solar receiver could be *simulated* by a controllable temperature profile along the reactor surface. Parametric effects of average reactor temperature, temperature distribution, residence time, steam-methane ratio are presented.

## EXPERIMENTAL FACILITY AND TEST SECTION

Reactor Test Section

Three main design considerations, noted below, were taken into account during the reactor test section design. The residence time within the channel had to be such that the reaction would not be carried out to completion; otherwise variations of input parameters would not be evident. Secondly, the channel had to be constructed to receive a longitudinally variable heat flux input. Thirdly, the reactor would need to be designed to withstand the elevated temperatures anticipated during the testing.

The final design of the reactor assembly is shown Figs. 1 and 2. Heat input was provided by nine Bernzomatic® torches impinging on the bottom surface of the reactor. The initial two torches acted as preheaters for the reactor, whereas
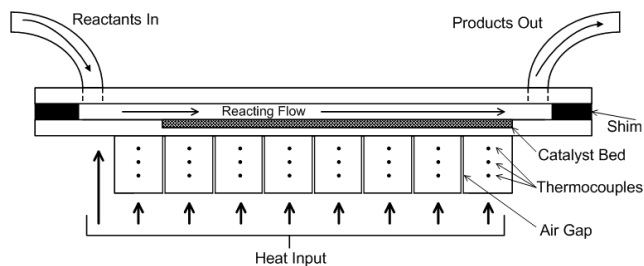
FIGURE 1. CROSS-SECTIONAL SCHEMATIC OF THE TEST SECTION
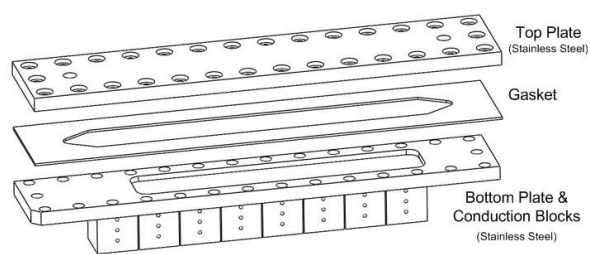
FIGURE 2. EXPLODED VIEW OF THE TEST SECTION

the subsequent seven torches impinged on the surface corresponding to the location of the catalyst and provided heat for the reaction. Half of the preheater zone had the same thermocouple arrangement as the catalyst zone, whereas in the other half the flame impinged directly on the reactor wall, thereby reducing heat transfer resistance. The microchannel height was formed by a high temperature gasket shim, compressed between two pieces of stainless steel to form a large aspect ratio channel. The Pd catalyst was contained on a porous FeCrAlY felt insert. The channel was held together with 30 8x32 stainless steel bolts distributed around the perimeter of the channel in order to distribute the compressive force as much as possible to minimize the potential for leaks in the system. To eliminate conduction between heating zones, 0.8 mm (1/32 in) air gaps separated each heating zone. The microchannel height was determined by measuring the thickness of the stainless steel walls forming the top and bottom of the reactor prior to assembly and subsequently measuring the thickness of the entire assembly after all bolts had been tightened. The catalyst bed was slightly taller than the cavity in the base of the reactor, causing the channel to be further restricted. The height of the catalyst bed used in this work was 3.175 mm (0.125 in). The final dimensions of the microchannel were 133.6 mm in length, 19 mm in width, and a height of 700 micrometers.

Experimental Facility

The minichannel reactor was integrated into a test facility as shown schematically in Fig. 3. Monitoring instrumentation is shown in green. Either N_2 or CH_4 could be routed through a switching valve and controlled using a common mass flow

TABLE 2. LIST OF INSTRUMENTATION

Item	Model	Range	Accuracy
Thermo-couples	OMEGA Super OMEGACLAD XL Type K KMTXL-062U-12 (Qty: 28)	0 - 1335 °C	+/- 0.4% of reading (>300°C)
Mass Flow Controller	Sierra Smart-Trak C100L	0 - 7 g/min	+/- 0.3% FS + 0.7% reading
Coriolis Meter	MicroMotion Elite CMF010 w/ MicroMotion 2700R Transmitter	0 - 50 g/min	+/- 0.05% of reading
Pressure Transducer	Validyne DP15-40 Transducer w/ Validyne CD15 Carrier Demodulator	0 - 345 kPa	+/- 0.25% of FS
USB-DAQ	NI USB-6009 DAQ	+/- 10 V	+/- 7.7 mV
DAQ	NI SCXI-1000 Chassis NI SCXI-1102 32 channel TC Amplifier NI SCXI-1303 Terminal block	+/- 10 V	0.05% of Reading
Gas Chromato-graph	HP 5890 with TCD	0 – 100 %	+/- 1.5% of reading
Scale	Scientech SA120	0 - 120 g	+/- 0.2 mg

controller. Deionized water was pressurized using a peristaltic pump capable of 689 kPa and controlled using a 16-turn needle valve. A Coriolis flow meter measured the water flow rate before it was injected into an evaporator. From the evaporator, the steam/gas mixture flowed through a 0.3 m insulated section to a 3 m (10 ft) coil of tubing situated on top of a 7.6 cm (3 in) diameter propane burner. This section (labeled as "Pre-heating and mixing coil" in Fig. 3) heats the gas mixture to near the inlet temperature (~550°C), and allows the gases time to premix via diffusion. The premixed, heated gases flowed through a short (~15 cm) section of insulated tubing configured with two monitoring ports (temperature & pressure) before flowing into the reactor. The product gases exited the reactor at a greatly elevated temperature (~700°C). A custom counter-flow shell and tube heat exchanger was used in order to decrease the exit gas temperature and condense water vapor in the product stream. The condensed water was drained from the heat exchanger and a relatively dry product stream was then directed either through a desiccant cartridge to remove any remaining water vapor and collected in sample bags for analysis in a gas chromatograph (GC), or vented to the atmosphere. Both exits were fitted with 20 gauge hypodermic needles. The needle situated after the desiccant cartridges was used for injection of the product gases into the sample bags, whereas the needle on the vent was used to provide uniform backpressure to the experiment regardless of whether the dry product gas was being collected or vented.
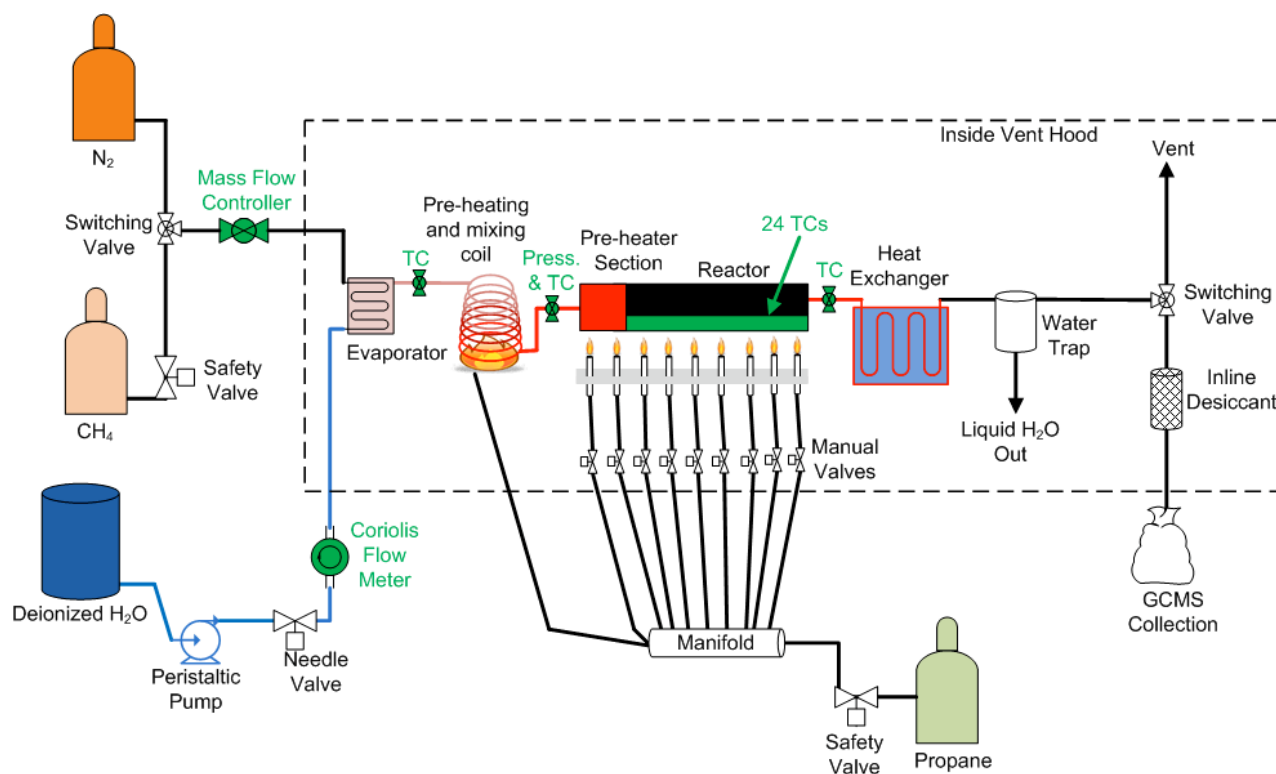
FIGURE 3. SCHEMATIC REPRESENTATION OF EXPERIMENTAL FACILITY

A propane cylinder was used to fuel all burners for approximately 12 hours. All propane delivery lines to the torches were unregulated and provided a variable temperature dependant pressure of 621 – 827 kPa. Each torch had a regulator, which provided a uniform pressure of 345 kPa to all torches. Several safety features were incorporated into the experimental facility. All high temperature components were located inside a fume hood. Two fire extinguishers were procured and located near the experiment. The CH_4 and propane feeds were fitted with 12 V normally-closed solenoid valves connected to a remote stop switch which was located near the laboratory exit. Experiments were only conducted when two or more people trained on the safety and experimental procedures were present.

Data were collected using two digital acquisition (DAQ) modules connected to a Windows PC running LabVIEW 8.5. A LabVIEW virtual instrument (VI) was developed which served to concatenate, display, and store all measured variables. All data were time-stamped using the time from the computer clock, and stored at a frequency of one hertz. Table 2 shows a list of instrumentation used along with their range and reported accuracies.

Catalyst Preparation

Palladium nanoparticle preparation. Palladium nano-particles were synthesized using a modified form of the

methods by Burst et al.[13,14]. To generate the palladium stock solution, 100 mg of palladium chloride was dissolved in 50 ml of 13 molar hydrochloric acid and diluted with deionized H_2O to 500 ml. Two drops (~40 mg) of dodecanethiol was added to 100 ml of toluene and poured into a round bottom flask. The flask was partially submerged in an ice bath and the mixture was stirred on a magnetic stirrer. Fifty milliliters of the stock palladium solution were added to the mixture along with 50 ml of deionized H_2O forming a biphasic mixture consisting of 100 ml aqueous phase and 100 ml organic phase. The solution was stirred rapidly for 30 minutes.

A reducing solution of 2 mg sodium borohydride and 40 ml deionized H_2O was prepared and situated above the mixture in a burette. The sodium borohydride solution was added dropwise to the mixture over a period of approximately 10 minutes. The mixture underwent a color change during the reduction process from light yellow to black, denoting the formation of palladium nanoparticles. The mixture was then stirred continuously for three hours during which the palladium nanoparticles were transferred from the aqueous phase to the organic phase. The aqueous phase was separated and discarded. Ten repetitions of this procedure were necessary to produce a batch of palladium nanoparticles. The resulting solution consisted of one liter of toluene containing nanoparticles produced from 100 mg of palladium chloride (60 mg palladium). This mixture was then evaporated under reduced pressure using a Buchi Rota-vapor R110 (Brinkman

5
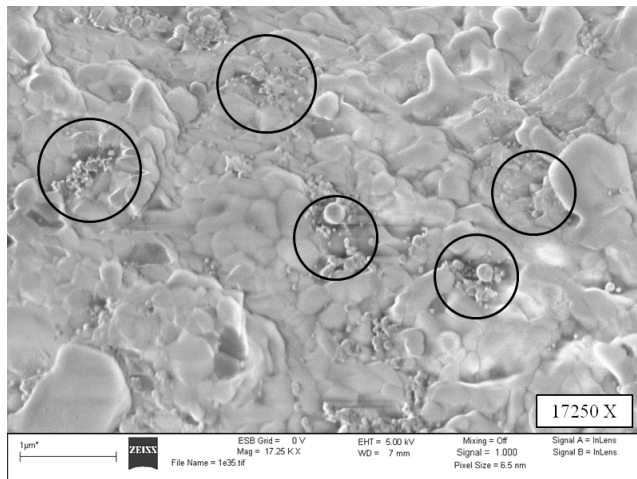
FIGURE 4. SEM IMAGE OF CATALYST BED AFTER FLOW SHEAR TESTING

Instruments, Westbury, NY). The original one liter of solution was evaporated to a volume of 40 ml of densely concentrated palladium nanoparticles suspended in toluene.

Catalyst Substrate and Nanoparticle Deposition. To enhance the surface area available for nanoparticle deposition, an 85% porous 3.175 mm (0.125 in) thick FeCrAlY metallic felt (FM542) provided by Technetics (www.techneticsfl.com), was used as a catalyst substrate for all experimental beds (except one, which was deposited directly onto the stainless steel channel wall). The FeCrAlY sheet was oxidized in a furnace at 900°C for four hours in an air environment, causing the aluminum to migrate to the surface and form α-alumina. This procedure has been documented to increase the surface area of the FeCrAlY by a factor of ten [15]. Scanning electron microscope (SEM) images taken of the substrate before and after the heat treatment process revealed an increase in surface area with the presence of a mixture of two different types of α-alumina (round nodules and thin ridges).

The aluminized felt was then cut to fit in the reactor and dried in an oven at 120°C for two hours to remove water vapor. The substrate was weighed using a Scientech SA 120 scale to establish an initial mass, then dip coated in the toluene/nanoparticle slurry. The catalyst bed used for the present experiments had an estimated Pd loading of 54 mg and was 133 mm in length. The bed was dip coated using a selective technique to enhance the percentage of catalyst present at the surface of the catalyst bed. A small amount of toluene solution containing concentrated Pd nanoparticles was poured into an aluminum block with a machined slot designed to accommodate a single catalyst bed. The catalyst bed was placed in the aluminum block to absorb the small amount of liquid onto a preferential side of the bed and the process repeated several times. The Pd-rich side of the bed formed the bottom wall of the microchannel. The catalyst impregnated

FeCrAlY was then dried at 110°C for two hours and weighed again to assess total mass loading.

Several small (19 mm x 10 mm) sections of aluminized FeCrAlY were loaded with catalyst for initial testing and characterization. One section was loaded into the reactor and exposed to a moderate temperature (500°C) high velocity (>10 m/s) flow of nitrogen to test for catalyst adhesion and durability (typical velocities during experiments were ~ 5 m/s). Particle sizes on the order of 15 nm were observed but a large degree of agglomeration occurred as can be seen in Fig. 4. The nanoparticles can be seen as the clumped small round particles distributed throughout both figures. No noticeable reduction in particle density was observed after the shear testing, suggesting that particles were adequately adhered to the substrate.

Catalyst Reduction. Reduction of noble metal catalysts is usually performed using a high temperature (350 – 800°C) stream of H_2 either in pure form or carried by an inert gas for a period of 1 – 3 hours [8,10,16,17]. Catalyst reduction for the present experiments utilized the same prescribed temperature regime as the work performed by Hou and Hughes [16] but a 4 % molar H_2/ 96 % Ar inert mixture was used as opposed to pure hydrogen used by Hou and Hughes [16].

The catalyst bed was situated in the reactor, and the reactor was assembled and configured inside the test loop. A N_2 stream was fed through the test loop and the reactor was heated to a temperature of 500°C and held constant for one hour. The feed gas was then switched to the H_2/Ar mixture and maintained at 500°C for two hours. The temperature of the reactor was then increased to 600°C and held for an additional hour. The feed gas was then switched back to N_2 and either experiments were conducted immediately, or the torches were turned off and the system was allowed to cool to ambient while maintaining the flow of nitrogen.

EXPERIMENTAL PROCEDURE

Prior to the start of each experiment, the gas valve was set to N_2 and the outlet valve was set to vent. The solenoid valves on the propane and CH_4 delivery lines were enabled. The instrumentation was then turned on. The mass flow controller was powered on and set to the desired flow rate, causing nitrogen to flow through the test loop. The evaporator was turned on and its temperature set using the PID controller. The LabVIEW VI was started on the computer and checked to ensure all inputs were being received properly. The main propane valve was then opened slowly and the pre-heater burner and torches were turned on. The neighboring torches were turned on in series and lit by the neighboring flame. The flow rate of each torch was adjusted so that the cone of the flame was just touching the surface of the reactor. The water valve to the heat exchanger was then turned on.

The reactor temperatures were monitored in LabVIEW. As the reactor temperatures approached the desired levels, the torch valves were adjusted individually to achieve the set

temperature at each heating zone to within 50°C. At this point the H_2O pump was turned on and the water valve was adjusted to the correct flow rate based on the CH_4 flow rate and the steam-methane ratio desired. The H_2O flow rate was continuously monitored throughout the experiment and adjusted if necessary. A significant increase in pressure was observed in LabVIEW, verifying that steam was flowing through the reactor. At this point the main CH_4 valve was opened and the regulator was set to 170 kPa. The gas valve was switched from N_2 to CH_4 and the experiment start time was recorded.

Minor adjustments were made to each torch to fine-tune the temperature in each heating zone. This process was ongoing throughout each experiment. The startup procedure generally required about 45 minutes. Reactor temperatures were regarded as stable once all measurements were within 10°C of the desired point for a period of three minutes.

Sampling of the outlet gases was conducted at different intervals depending on which tests were being performed, but the general procedure remained the same. Two minutes prior to the expected sample time the outlet valve was switched to direct the flow through the desiccant cartridges. The volume of each desiccant cartridge was on the order of 50 ml, and it was desired to completely flush the contents of previous experiments. The outlet terminated at a section of tubing that was fitted with a hypodermic needle, through which all outlet gases passed. At the desired time, the needle was inserted into the septum on the sampling bag. The sample bag was allowed to fully inflate, at which point the needle was removed. The outlet valve was then switched back to vent to reduce the water vapor load through the desiccant.

After all samples had been collected, a set sequence of steps was performed to ensure that the catalyst was not damaged. To begin the shutdown procedure, the gas flow was switched from CH_4 to N_2. The main tank valve on the CH_4 tank was turned off. The H_2O flow was stopped by turning off the pump. Data collection in LabVIEW was stopped, but the program was kept running in order to monitor temperatures. The main propane valve was turned off, as were both solenoid valves. The pre-heater burned was then turned off, followed by the evaporator. Time was allowed for the propane torches to burn off the residual gas present in the delivery lines, after which all propane torch valves were closed. The water flow to the heat exchanger was then stopped. Approximately two hours was required for the reactor to cool to near ambient temperature at which pont the flow of N_2 was stopped.

DATA REDUCTION AND UNCERTAINTY ESTIMATES

The steam-methane ratio was calculated using the molar flow rates as

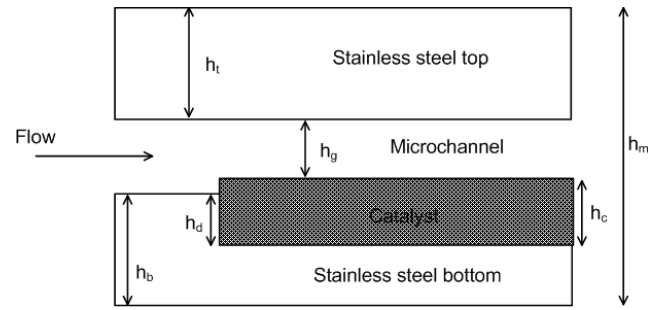$$R_{SM} = \frac{\dot{M}_{H_2O}}{\dot{M}_{CH_4}} \qquad (4)$$

FIGURE 5. CHANNEL HEIGHT ESTIMATION

where the molar flow rates of component i, $\dot{M}_i$ are calculated using the mass flow rate of component i and the molecular weight of component i,

$$\dot{M}_i = \frac{\dot{m}_i}{M_i} \qquad (5)$$

The residence time is estimated as

TABLE 3. UNCERTAINTIES IN MEASURED VARIABLES

Parameter	Calibration Uncertainty	Stability Uncertainty	Total Uncertainty
Temperature	0.20%	0.64%	0.67%
Pressure	350 Pa	138 Pa	376 Pa
H_2O Flow Rate	0.0029 g/min	0.050 g/min	0.050 g/min
CH_4 Flow Rate	0.021 g/min + 0.7%	0.9%	0.021 g/min + 1.1%
H_2%	4.99%	0.47%	5.01%
CO%	6.57%	0.44%	6.58%
CH_4%	1.95%	0.11%	1.95%
CO_2%	5.30%	1.71%	5.57%
Thermocouple separation			0.01 mm
All caliper measured distances (l, w, h)			0.05 mm

TABLE 4. UNCERTAINTIES IN DETERMINED VARIABLES

Parameter	Uncertainty
Surface Temperature, T_s	2.13%
Microchannel Height, h_g	0.11 mm
Residence Time, t_{res}	17.3%
Steam-Methane Ratio, R_{SM}	14.9%

$$t_{res} = \frac{l}{U} \qquad (6)$$

where l is the length of the channel with catalyst and U is the cross-sectional average velocity of flow in the channel. The average velocity is calculated based on the mixture-averaged volumetric flow rate and open channel cross-sectional dimensions,

$$U = \frac{\dot{V}}{w \cdot h} \qquad (7)$$

The volumetric flow rate is determined as

$$\dot{V} = \sum_i \frac{\dot{m}_i}{\rho_i} \qquad (8)$$

The surface temperature at each axial location in the channel is estimated based on the vertically located thermocouples as shown in Fig. 1 using a one-dimensional heat conduction model,

$$T_s = T_{lower} + \frac{(T_{upper} - T_{lower})}{\Delta x_{upper-lower}} \cdot \Delta x_{surface-lower} \qquad (9)$$

The microchannel height was determined as shown in Fig. 5 using five measurements using a caliper,

$$h_g = h_m - (h_t - h_b) - (h_c - h_d) \qquad (10)$$

Calibrations were conducted on thermocouples, pressure sensor, Coriolis flow meter, and gas chromatograph. The factory calibration was used for the Sierra mass flow meter. Table 3 presents a summary of the typical uncertainties in measurements using relevant instruments. These uncertainties were calculated using the root sum squared (RSS) method and estimated based on calibration uncertainties and standard deviation during experiments, which represented the system stability. Sequential perturbation of dependant parameters by their corresponding uncertainties was used to generate uncertainties for the most important parameters of this study [18]. The results are shown in Table 4. The perturbations were conducted for a sample with a methane flow rate of 0.194 g/min, steam-methane ratio of 3, and reactor temperature near 850°C. The majority of the uncertainty of the surface temperature is associated with stability during operation. The large microchannel height uncertainty is due to it being a function of five measurements conducted with hand calipers with a bias uncertainty of 0.05 mm. The residence time uncertainty is almost entirely attributed to the uncertainty of the channel height. Uncertainties for the steam-methane ratio

decrease at higher flow rates due to the absolute accuracy of the mass flow controller.

TABLE 5. EXPERIMENTAL MATRIX

Varied Parameter	t_{res} (ms)	$\dot{m}_{CH_4}$ (g/min)	T_s (°C)	R_{SM}	P (kPa-abs)
Catalyst stability	24.1 - 26.0	0.194	854 - 874	2.86 - 3.05	105 - 108
t_{res}	5.3 - 34.1	0.15 - 1.40	777 - 783	2.91 - 3.15	106 - 162
T_s	24.8 - 27.3	0.183 - 0.233	625 - 904	2.87 - 3.13	105 - 108
T_s profile	25.7 - 29.6	0.194	748 - 759	3.01 - 3.07	108
R_{SM}*	24.7- 27.2	0.15- 0.3	817- 825	2.54- 5.80	112- 120

*a catalyst bed with uniform distribution of Pd on both sides of the substrate was used for this study

RESULTS AND DISCUSSION

Catalyst stability was tested over 4 hours of run time at an average reactor surface temperature of approximately 864 °C, a steam-methane ratio (R_{SM}) of 2.95 and a residence time of 25 ms. H_2 production reached a stable value of around 35 percent after 100 minutes of testing. Results from parametric variations of residence time, average reactor temperature, and reactor axial temperature profile are presented in the sections following. Effect of variation of steam-methane ratio on hydrogen yield was studied using a different catalyst bed and results for this parametric variation are presented at the end. Table 5 presents a listing of the experimental conditions for results presented in the following sections.

Residence Time Variation

The effect of variation of residence time, as defined in Eq. 6, on hydrogen production is presented in this section. Table 5 provides the experimental conditions for this study. The residence time was manipulated by changing the flow rate of both the steam and methane such that the steam-methane molar ratio was maintained constant. No backpressure was applied to the system, consequently the inlet pressure increased for the higher flow rates. All heating torches were set to impinge on the heating surface at approximately the same intensity and a steady state surface temperature profile was allowed to develop. The temperature profile along the reactor is shown in Fig. 6. The decreasing trend in temperature along the channel is due to higher conduction and radiation losses near the exit of the channel.

The dry output gas concentrations are shown in Fig. 7. The trend is linear up to a conversion of about 20 percent and the intercept of the trend line goes to the origin. There was a slight decrease from the linear trend of hydrogen production with increase in residence time. This can be attributed to the partial pressure of methane being reduced from the conversion

process, thereby providing diminishing returns for additional residence time. This effect was seen in H_2 concentrations above 20 percent.

Low conversion rates would correspond with large velocities or small reactor lengths, such that the combination of diffusion time for reactants and product gases to and from the catalyst wall and the reaction time are in excess of the residence time.

Figure 8 shows a plot of estimated diffusion times as a function of reactor temperature. The diffusion time is estimated as

$$t_{diff} = \frac{h_g^2}{D} \quad (11)$$

where the diffusion coefficient D was calculated using the formula from Kuznetsov and Kozlov [19], which is a simplified version of the work outlined by Fuller (1969) [20],

$$D = \frac{9.99 \cdot 10^{-5} T^{1.75}}{P} \quad (12)$$

For the present microchannel of 0.7 mm height, diffusion times varied from 6 ms for a temperature of 400 ^{o}C to 2 ms for a reactor temperature of 900 ^{o}C. Since the diffusion time is of similar order as the residence time, especially for the higher velocity flows, higher conversions can be achieved by lowering the velocity or by reducing the channel size. Since the diffusion times are about an order of magnitude smaller for residence times in excess of 30 ms, conversion is not limited by diffusion for larger residence times.

Reactor Temperature Variation

The overall reaction rate has an Arrhenius-type exponential dependence on temperature; consequently temperature is expected to have a strong effect on methane conversion. Values of variables for this parametric study are provided in Table 5. Calculations were performed prior to the experiment in order to determine the flow rates necessary to operate at a set residence time due to the variations of density with temperature. The temperature profiles in this experiment were maintained
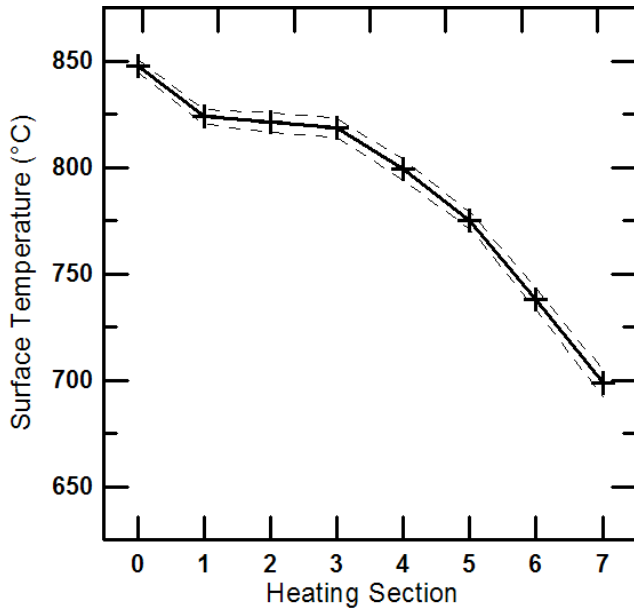

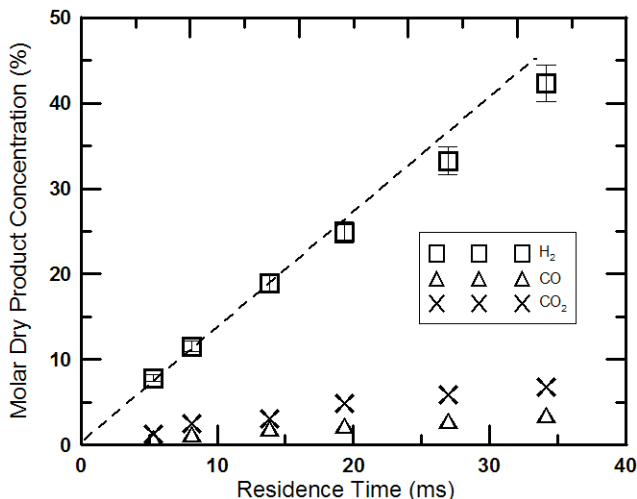**FIGURE 6.** TEMPERATURE PROFILE ALONG THE REACTOR FOR VARIED RESIDENCE TIME STUDIES

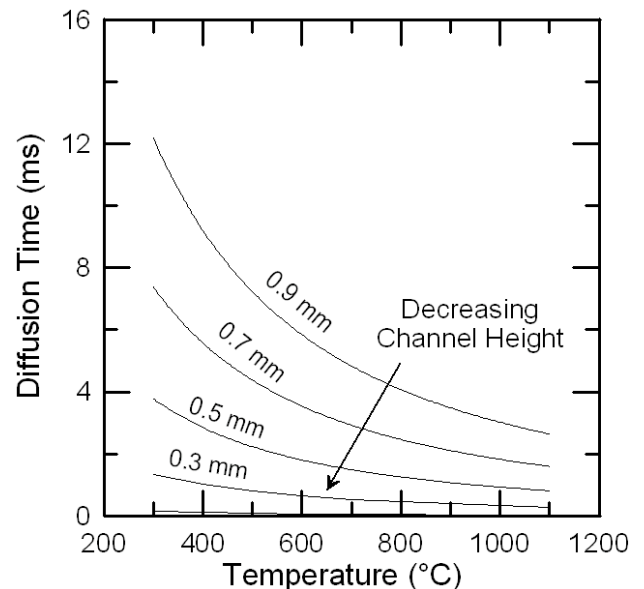**FIGURE 7.** DRY PRODUCT MOLAR CONCENTRATION AS A FUNCTION OF RESIDENCE TIME

FIGURE 8. ESTIMATED DIFFUSION TIMES AS A FUNCTION OF TEMPERATURE FOR DIFFERENT MICROCHANNEL HEIGHTS

approximately uniform as the effect of reactor temperature change needed to be observed. Figure 9 depicts the temperature profile along the reactor and Fig. 10 shows the corresponding dry product outlet concentrations. As can be seen an exponential dependence of hydrogen production on reactor surface temperature is observed.

Figure 11 presents the CO selectivity, expressed as the ratio of CO to the sum of CO and CO_2 on a molar basis, as a function of reactor temperature. The CO selectivity showed a strong positive correlation with temperature at temperatures greater than 700°C. An increased CO selectivity indicates lower rates of the exothermic water-gas shift reaction, Eq. 2. Alkhaldi [10] also observed a strong correlation of CO selectivity and temperature over a Pd catalyst; the results of which are plotted alongside the current experimental data. The CO selectivities seen in this work were generally lower than those seen by Alkhaldi [10]. The data of Alkhaldi

FIGURE 9. TEMPERATURE PROFILE ALONG THE REACTOR FOR VARIED REACTOR SURFACE TEMPERATURE STUDIES

FIGURE 10. DRY PRODUCT MOLAR CONCENTRATION AS A FUNCTION OF REACTOR SURFACE TEMPERATURE
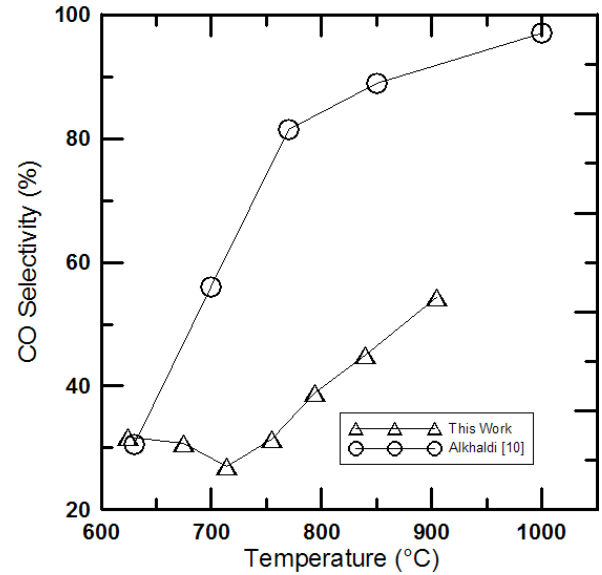
FIGURE 11. VARIATION OF CO SELECTIVITY WITH TEMPERATURE

correspond to a residence time of 27.9 ms at a reactor temperature of 1000 °C and a residence time of 39.3 ms at T=630 °C. The steam-methane ratio for Alkhaldi's data was 4.83.

Axial Temperature Profile Variation

Experiments were conducted to explore the influence of temperature distribution along the reactor. Experimental conditions are listed in Table 5 and include a fixed residence time of ~27 ms and a steam-to-methane ratio of 3. The configuration was such that the average temperature of the reactor was held constant at 750°C, but the longitudinal temperature profiles were varied across four different ramp configurations as shown in Fig. 12.

Two flat profiles were tested, one at the start and one at the end of the experiment to check for consistency. Two "ramp up" and two "ramp down" profiles were studied; one with a temperature difference of 100°C from the entrance of the reactor to the exit, and one with a difference of 200°C, for a total of four ramping configurations. It was expected that the Ramp Down 200 temperature profile would exhibit the highest conversion rate due to the greatly elevated temperatures (and reaction rates) at the inlet, where the partial pressure of methane was greatest. The gas chromatograph output from the experiment is plotted in Fig. 13. All ramping scenarios produced a significantly higher percentage of hydrogen than the flat line profiles. About a 46 percent increase in yield of hydrogen is obtained by ramping profiles compared to the flat profile condition. For the Ramp Down profiles, the higher temperature ramp (Ramp Down 200) results in a slightly higher hydrogen yield than the Ramp Down 100 condition. For the Ramp Up profiles, the output hydrogen concentrations were
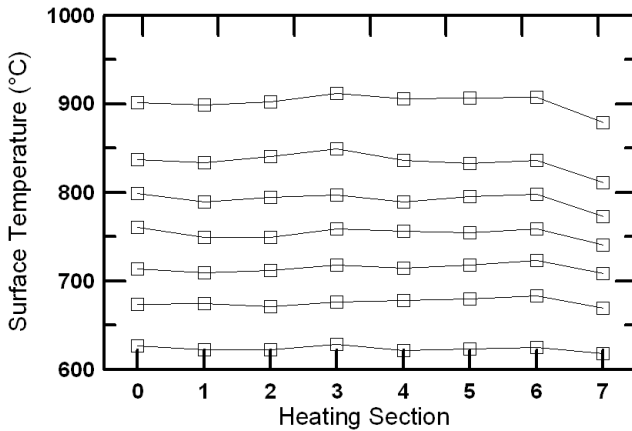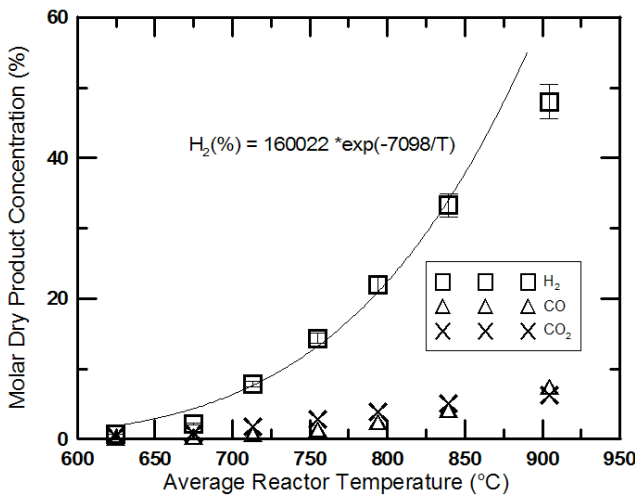
within limits of uncertainty so the individual effects of ramping profiles cannot be contrasted. The most significant result from this parametric study is that it is more desirable to maintain a portion of the reactor at a high temperature and the rest of the reactor at a lower temperature than to have the reactor that is at an average temperature equal to that of the ramp case.

Molar Steam-Methane Ratio Variation

The effect of variation of steam-methane ratio on hydrogen yield keeping all other parameters constant was performed. For

FIGURE 12. AXIAL TEMPERATURE DISTRIBUTION WITH A FIXED AVERAGE SURFACE TEMPERATURE

FIGURE 13. DRY PRODUCT MOLAR CONCENTRATION FOR VARIOUS SURFACE TEMPERATURE PROFILES

this experiment, a slightly different variation of catalyst bed was used. While the Pd catalyst was prepared in exactly the same manner as for the one previously reported, the distribution of catalyst on the aluminized substrate was different. The same amount of Pd nanoparticles were dip coated without any preferential loading on one side of the substrate as was done for the previous catalyst bed.

Experimental conditions are listed in Table 5. The residence time was kept constant around 26 ms and the average surface temperature of the reactor was 821 $^{\circ}$C. Steam methane ratio was varied between 2.5 and 6. Rapid catalyst deactivation can occur at lower steam-methane ratios due to coke formation. In order to avoid this, the lowest steam-methane ratio tested was limited to 2.5. The advantages of using a smaller steam-methane ratio would be decreased energy costs of heating the steam and increased residence times for a given methane flow rate. The flow rate of methane and steam were adjusted in order to keep the residence time through the reactor near constant. The temperature profile used during this experiment is shown
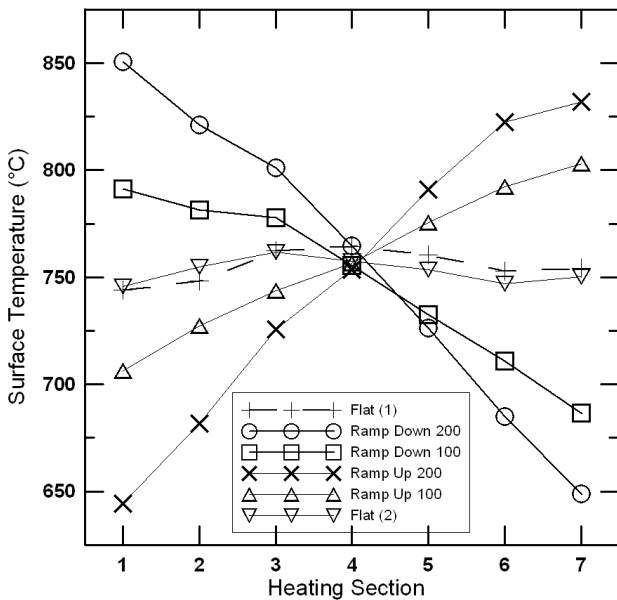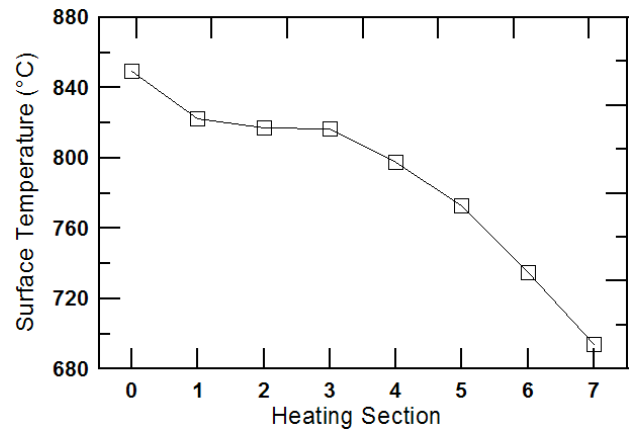
FIGURE 14. TEMPERATURE DISTRIBUTION ALONG THE REACTOR FOR R_{SM} STUDY
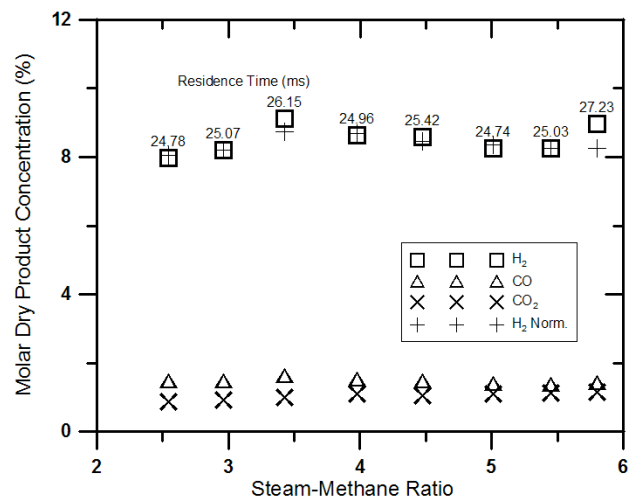
FIGURE 15. DRY PRODUCT MOLAR CONCENTRATION FOR STEAM-TO-METHANE MOLAR RATIOS

in Fig. 14.

The molar output percentages are plotted in Fig. 15. Little difference was observed amongst sample points, with variations in output corresponding well to slight changes in residence time. The H_2 molar concentrations were linearly scaled to a residence time of 25 ms using

$$y_{H_2, t_{res} 25ms} = y_{H_2, exp} \frac{25 \ (ms)}{t_{res} \ (ms)} \qquad (13)$$

where $y_{H_2, exp}$ is the molar concentration of H_2 and t_{res} is the residence time in milliseconds. By normalizing the H_2 concentrations, several of the outlying points were brought closer to a straight line (see the + symbols), suggesting that the steam-methane ratio has little to no effect on the H_2 output under the conditions tested.

CONCLUSIONS

An experimental study of steam-methane reforming in a large aspect ratio microchannel is presented. Palladium nanoparticles, deposited on aluminized FeCrAlY, were used as a catalyst for the reactions. Parametric studies of residence time, average surface temperature, surface temperature profiles, and steam-to-methane ratio were performed. Results from the residence time study indicates an increase in molar hydrogen output with increasing residence time, indicating that the sum of the diffusion and reaction times are larger than residence times for all conditions tested. Hydrogen yield is seen to increase exponentially with reactor temperature. A down-ramping temperature profile with the same average temperature as a uniform or ramp-up profile increased hydrogen production. Steam-to-methane molar ratio variation did not have a significant affect on hydrogen yield in the range of the present experiments.

ACKNOWLEDGMENTS

REFERENCES

[1] Rostrup-Nielsen J. R., and Rostrup-Nielsen T., 2002, "Large-Scale Hydrogen Production," CATTECH, **6**(4), pp. 150-159.

[2] Chaniotis A., and Poulikakos D., 2005, "Modeling and optimization of catalytic partial oxidation methane reforming for fuel cells," Journal of Power Sources, **142**(1-2), pp. 184-193.

[3] Pregger T., Graf D., Krewitt W., Sattler C., Roeb M., and Möller S., 2009, "Prospects of solar thermal hydrogen production processes," International Journal of Hydrogen Energy, **34**(10), pp. 4256-4267.

[4] Rostrup-Nielsen J. R., Sehested J., and Norskov J. K., 2002, "Hydrogen and Synthesis Gas by Steam and CO2 Reforming," Advances in Catalysis, **47**, pp. 65-139.

[5] Kolb G., and Hessel V., 2004, "Micro-structured reactors for gas phase reactions," Chemical Engineering Journal, **98**(1-2), pp. 1-38.

[6] Holladay J. D., Wang Y., and Jones E., 2004, "Review of Developments in Portable Hydrogen Production Using Microreactor Technology," Chemical Reviews, **104**(10), pp. 4767-4790.

[7] Tonkovich A., Perry S., Wang Y., Qiu D., LaPlante T., and Rogers W., 2004, "Microchannel process technology for compact methane steam reforming," Chemical Engineering Science, **59**(22-23), pp. 4819-4824.

[8] Wang Y., Chin Y., Rozmiarek R., Johnson B., Gao Y., Watson J., Tonkovich A., and Vander Wiel D., 2004, "Highly active and stable Rh/MgOAl2O3 catalysts for methane steam reforming," Catalysis Today, **98**(4), pp. 575-581.

[9] Cao C., Wang Y., and Rozmiarek R. T., 2005, "Heterogeneous reactor model for steam reforming of methane in a microchannel reactor with microstructured catalysts," Catalysis Today, **110**(1-2), pp. 92-97.

[10] Alkhaldi K. H., 2005, Steam Reforming of Hydrocarbons in a Microreactor: Experiment and Modeling, Ph. D. Thesis, Oregon State University.

[11] Tonkovich A. L. Y., Yang B., Perry S. T., Fitzgerald S. P., and Wang Y., 2007, "From seconds to milliseconds to microseconds through tailored microchannel reactor design of a steam methane reformer," Catalysis Today, **120**(1), pp. 21-29.

[12] Johnson B. R., Canfield N. L., Tran D. N., Dagle R. A., Li X. S., Holladay J. D., and Wang Y., 2007, "Engineered SMR catalysts based on hydrothermally stable, porous, ceramic supports for microchannel reactors.," Catalysis Today, **120**(1), pp. 54-62.

[13] Valmikanathan O., Ostroverkhova O., Mulla I., Vijayamohanan K., and Atre S., 2008, "The effect of synthesis procedure on the structure and properties of palladium/polycarbonate nanocomposites," Polymer, **49**(16), pp. 3413-3418.

[14] Brust M., Bethell D., Kiely C. J., and Schiffrin D. J., 1998, "Self-Assembled Gold Nanoparticle Thin Films with Nonmetallic Optical and Electronic Properties," Langmuir, **14**(19), pp. 5425-5429.

[15] Aartun I., 2004, "Catalytic conversion of propane to hydrogen in microstructured reactors," Chemical Engineering Journal, **101**, pp. 93-99.

[16] Hou K., and Hughes R., 2001, "The kinetics of methane steam reforming over a Ni/α-Al2O catalyst," Chemical Engineering Journal, **82**(1-3), pp. 311-328.

[17] Aartun I., Gjervan T., Venvik H., Görke O., Pfeifer P., Fathi M., Holmen A., and Schubert K., 2004, "Catalytic

conversion of propane to hydrogen in microstructured reactors.," Chemical Engineering Journal, **101**(1-3), pp. 93-99.

[18]   Moffat R. J., 1985, "Using Uncertainty Analysis in the Planning of an Experiment," J. Fluids Eng., **107**(2), pp. 173-178.

[19]   Kuznetsov V., and Kozlov S., 2008, "Modeling of methane steam reforming in a microchannel with a heat flow distributed in length," Journal of Engineering Thermophysics, **17**(1), pp. 53-59.

[20]   Fuller E. N., Ensley K., and Giddings J. C., 1969, "Diffusion of halogenated hydrocarbons in helium. The effect of structure on collision cross sections," The Journal of Physical Chemistry, **73**(11), pp. 3679-3685.